Mechanism of Macroscopic Motion of Oleate Helical Assemblies: Cooperative Deprotonation of Carboxyl Groups, Triggered by Photoisomerization of Azobenzene Derivatives

Yoshiyuki Kageyama,* Tomonori Ikegami, Yuta Kurokome, and Sadamu Takeda*
Chemistry — A European Journal **2016**, *22(25)*, 8669–8675.
DOI: 10.1002/chem.201600426

FULL PAPER

In photo-triggered macroscopic motions of hybrid assemblies of oleic acid and an azobenzene derivative, photoisomerization-coupled deprotonation was observed.

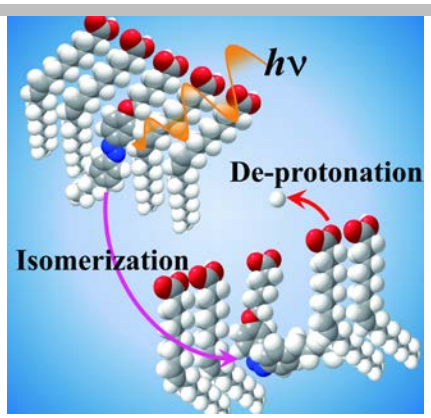

Y. Kageyama, T. Ikegami, Y. Kurokome, and S. Takeda**

Page 8669 – Page 8675

Mechanism of Macroscopic Motion of Oleate Helical Assemblies: Cooperative Deprotonation of Carboxyl Groups, Triggered by Photoisomerization of Azobenzene Derivatives

Yoshiyuki Kageyama,* Tomonori Ikegami, Yuta Kurokome, and Sadamu Takeda*
Chemistry — A European Journal 2016, 22(25), 8669–8675. (DOI: 10.1002/chem.201600426)

Mechanism of Macroscopic Motion of Oleate Helical Assemblies: Cooperative Deprotonation of Carboxyl Groups, Triggered by Photoisomerization of Azobenzene Derivatives

Yoshiyuki Kageyama,*[a,b] Tomonori Ikegami,[c] Yuta Kurokome,[c] and Sadamu Takeda*[a]

Abstract: We previously reported azobenzene-photoisomerization-induced macroscopic and spatially ordered motions of self-assemblies composed of oleic acid and a small amount of an azobenzene derivative. However, the mechanism of the generation of submillimeter-scale motions by the nanosized structural transition of azobenzene has not been clarified. In this paper, we propose an underlying mechanism of the motions, where the cooperative deprotonation of carboxylic acids in conjunction with azobenzene photoisomerization results in the morphological transition of the self-assembly, which, in turn, results in macroscopic forceful dynamics. The photoinduced deprotonation was investigated by potentiometric pH titrations and Fourier transform infrared spectroscopy. We expect the concept of hierarchical molecular interaction generating macroscale function to promote the next stage of supramolecular chemistry.

Introduction

The development of molecular motions for macroscopic dynamics is a key step for creating artificial supramolecular machines.[1] Numerous materials that undergo photoinduced macroscopic motions have already been prepared.[2] For example, photoinduced bending of crystalline assemblies composed of photochromic compounds such as diarylethene derivatives[3] or a salicylideneaniline derivative[4] have been reported. Photoinduced isomerizations of azobenzene dyes have frequently been employed. The large changes induced in the steric structure, effective volume, and dipole moment of the azobenzene moiety by photoisomerization enable macroscopic motions of crystals[5] and polymers.[6] Recently, macroscopic self-oscillatory motions of a co-crystal[7] and polymers[8] under continuous photoirradiation have been reported. The self-organized motion of the co-crystal is interesting not only from the viewpoint of repetitive photomechanical motion but also with regard to the relationship between its dissipative dynamics in a far-from-equilibrium state and life phenomena. Another interesting aspect of photoinduced motions of noncovalent assemblies is their characteristic transitions enabled by the soft association among molecules.[9] For example, Higashiguchi *et al.* reported the photoinduced reversible motion of an amphiphilic diarylethene derivative that exhibited a morphological transition between a spherical assembly and a fibril assembly via photoisomerization.[10] Hamada *et al.* reported the budding motion of azobenzene-containing phospholipid vesicles and the opening–closing dynamics of spherical membranes.[11] To enable a wide variety of motions, mechanistic investigations of mechanical transitions of soft and noncovalent self-assemblies are now desired.

We previously reported the macroscopic motions of lyotropic assemblies composed of oleic acid and a minor amount of amphiphilic azobenzenes.[12] We demonstrated three types of motion: expansion of a vesicular membrane, morphological transformation from a bold helical assembly to straightened rod-like assembly, and a recoiling–coiling motion of a tightly coiled helical assembly. All of these motions were reversible under irradiation with alternating light wavelengths between 366 nm and 435 nm. After the publication of this study, we observed that the helical assemblies are constructed by a hexagonal bundling of inverted tubular micelles, as revealed by synchrotron microbeam small-angle X-ray diffraction (μSAXD) analysis (the *d*-spacing was 5.47 nm).[13] In this paper, we demonstrate another forceful motion exhibited by tightly coiled thin helical assemblies: a tail-shaking motion with recoiling. Furthermore, we propose an underlying mechanism for these photoactivated macroscopic motions, in which the cooperative deprotonation of a carboxylic acid moiety is induced by the azobenzene photoisomerization.

Results and Discussion

pH-dependent self-assembly behavior of oleic acid

In aqueous media, sodium oleate (**1Na**, Figure 1) self-associates into assemblies of several shapes in a pH-dependent manner.[13,14] Such formation of pH-dependent assemblies of several shapes is due to the ratio of the protonated form (**1H**) to the anion form ($\mathbf{1}^-$). Figure 2 summarizes the characteristic quasi-stable morphologies of oleate liquid crystalline assemblies at various pH levels at 25 °C, as demonstrated by a pH titration curve of 6.6 mM **1Na**, which was reported in our previous work.[13] In addition to the assemblies shown in Figure 2, invisible spherical micelles exist in the dispersion, and crystalline assemblies are also formed by cooling.[14f,g] Because the morphology of each assembly also depends on its assembling history, we can observe multi-shape assemblies in the same dispersed solution. According to the pH titration curve measured under vigorous stirring, the apparent pK_a is 7.5, which is higher than those of water-soluble fatty acids, which typically exhibit pK_a values of approximately 4.8. The difference in the curve of **1Na** from that of water-soluble fatty acid arises from the consequences of self-association, which include an increase in

[a] Dr. Y. Kageyama and Prof. Dr. S. Takeda
Department of Chemistry, Faculty of Science
Hokkaido University
North-10, West-8, Sapporo, 060-0810, Japan
E-mail: y.kageyama@mail.sci.hokudai.ac.jp,
Fax: +81-11-706-4841
stakeda@sci.hokudai.ac.jp
[b] Dr. Y. Kageyama
JST PRESTO
[c] Mr. T. Ikegami and Mr. Y. Kurokome
Graduate School of Chemical Sciences and Engineering
Hokkaido University

Supporting information for this article is given via a link at the end of the document.

electric repulsion between the self-assembled carboxylates and a decrease in permittivity and proton activity of the surface water surrounding the self-assemblies.[14b,c,15] Moreover, the winding and slow slope of the titration curve of **1Na** between pH 6.8 and 7.8 indicates that the protonation properties of **1Na** depend on the shapes of the self-assemblies. In this narrow pH range, the morphology of self-assemblies and the ratio of **1H** to $\mathbf{1}^-$ in each self-assembly changes dramatically. Self-assemblies of these shapes are capable of being formed in a mixed dispersion of **1Na** and 10%(w/w) of an amphiphilic azobenzene derivative (6-[4-(4-*n*-butylphenylazo)phenoxy]hexanoic acid, **2**)[7a,12] prepared under dark conditions, even if the pH value and molar ratio slightly differ from those of dispersions without **2**.

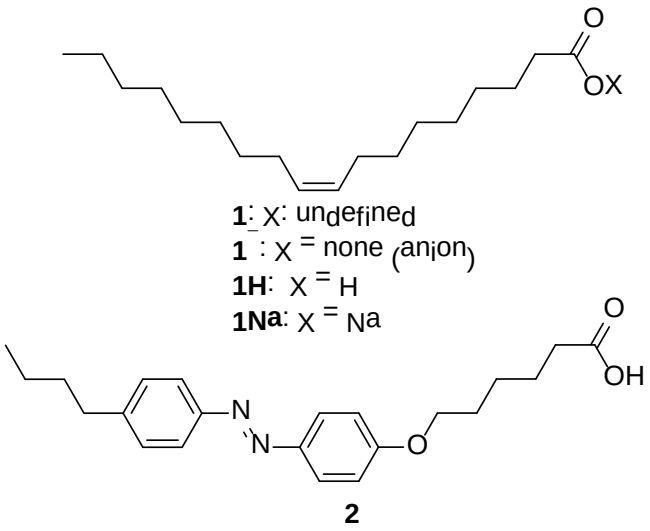

Figure 1. Structures of sodium oleate (**1Na**), its derivatives, and amphiphilic azobenzene **2**.

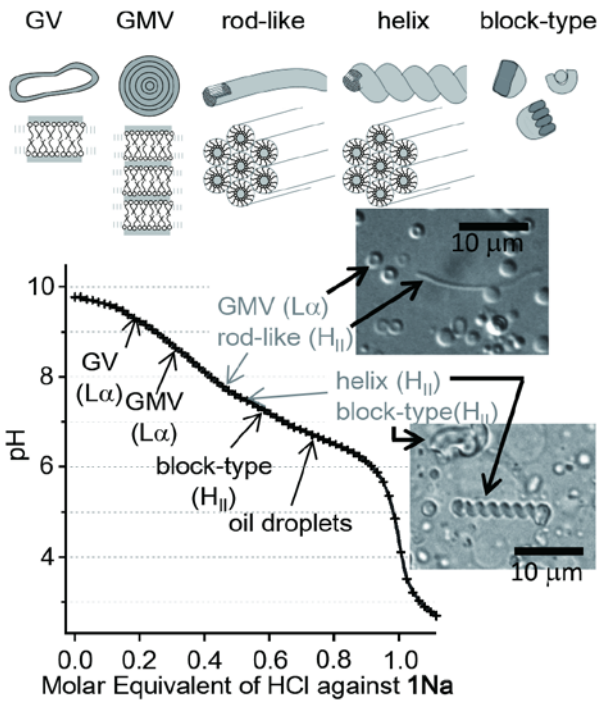

Figure 2. pH titration curve for the titration of **1Na** by HCl (aq) and illustrations of the macroscopic assemblies formed at the respective pH levels based on microscopic observation and microbeam small-angle X-ray diffraction measurements.[13] Abbreviations in the figure are as follows: GV (giant vesicle), GMV (giant multilamellar vesicle), Lα (lamellar phase), and H_{II} (inverted hexagonal phase).

Macroscopic motions of assemblies composed of oleic acid and an amphiphilic azobenzene derivative

In our previous paper, we demonstrated reversible macroscopic motions induced by photoirradiation of various self-assemblies composed of **1Na** and **2** (10%(w/w) for **1Na**): an enlargement of the vesicular membrane at pH 7.8, a helix-to-rod transformation at pH 7.5, and a helix-to-helix transformation with propelling motion at pH 7.4, were observed under irradiation with 365-nm light, and their reverse transformations were observed under irradiation with 435-nm light.[12] This reversibility indicates that the morphological changes were induced not by the thermal phase transition of the assemblies due to the light absorption but by the photoinduced isomerization of **2**. In the present study, we demonstrate another forceful motion, as observed by difference interference microscopy, under irradiation with 365-nm light from a high-pressure mercury lamp installed on the microscope. Tightly coiled thin helical assemblies at pH 7.5 exhibited a tail-shaking motion with recoiling, and the length of the helix decreased to the point where the assemblies became invisible (Figure 3; Movie S1 in supporting information (SI)). Despite subsequent photoirradiation with 435-nm light, no assemblies were recovered. Therefore, the tail-shaking with recoiling motion is a result of a transition from a helical assembly to invisible small assemblies such as spherical micelles.

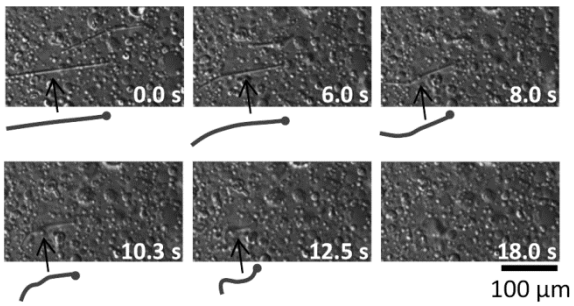

Figure 3. Photoactivated tail-shaking motion of a tightly coiled thin helical assembly composed of **1** and **2**.

Conversely to the forceful motion of self-assemblies composed of **1** and **2**, only small motions were observed in both vesicles and multilamellar tubes (so-called myelin figure) composed of egg-yolk lecithin and 10%(w/w) of **2**; the vesicular assemblies slightly enlarged via a transition oval sphere, and helical myelin figures expanded their length slightly under UV-light irradiation, as shown in Figures S1 and S2 in the SI.

To elucidate the universal mechanism responsible for these aforementioned and previously reported photoinduced motions, we investigated the changes in various properties of assemblies before and after photoirradiation.

Π–A curve measurement of mixed monolayer

According to Hamada et al.,[11b] the membrane surface area composed of dioleoylphosphatidylcholine and the amphiphilic azobenzene named KAON12 (6:4 in molar ratio) expanded by

11% under UV irradiation. They attributed this expansion to the increase in the molecular cross-sectional area of KAON12 by photoisomerization and concluded that increase in the membrane area by photoirradiation leads to budding motions of vesicles. Using the Wilhelmy plate method,[16] we measured the surface pressure–area (Π–A) profiles of monolayers composed of oleic acid (**1H**, 16.2 nmol (90%)) and **2** (1.8 nmol (10%)) spread over distilled water in dark or under 365-nm light irradiation using a UV-LED (Figure 4). The areas of individual-molecules were calculated by dividing the monolayer area by the sum of molecular numbers of **1H** and **2**. The limiting areas (A_0s), estimated from linear slopes shown in Figure 4 were 0.43(4) nm^2 and 0.45(4) nm^2 for under dark condition and light irradiation, respectively.[17] Given that the A_0 of the purchased **1H** was 0.44 nm^2 when measured under the same conditions,[18] the 365-nm light irradiation changed the limiting cross-sectional area of **2** in the mixed monolayer from approximately 0.35 nm^2 to 0.55 nm^2 (value in photostationary state). Even the increase in the cross-sectional area of **2** by *trans*-to-*cis* photoisomerization was large, and the 4.6% increase in the area of the mixed monolayer is assumed to be too small to account the observed forceful motions of assemblies. Thus, a more essential mechanism must operate in concert with this increase in the molecular area of **2**.

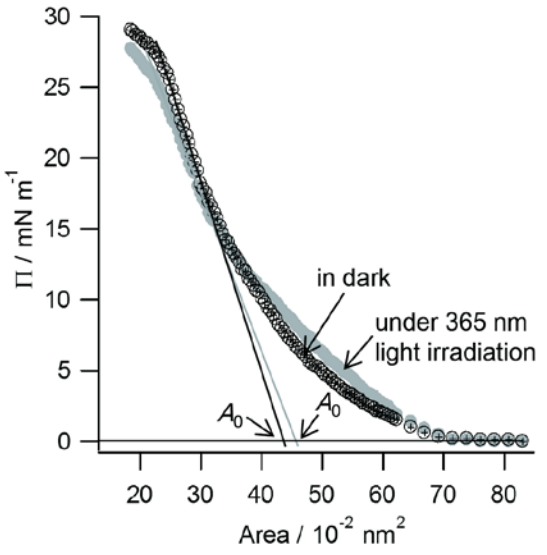

Figure 4. Surface pressure–area (Π–A) plots for mixed monolayers of **1H** (90%) and **2** (10%) measured in the dark and under 365-nm light irradiation.

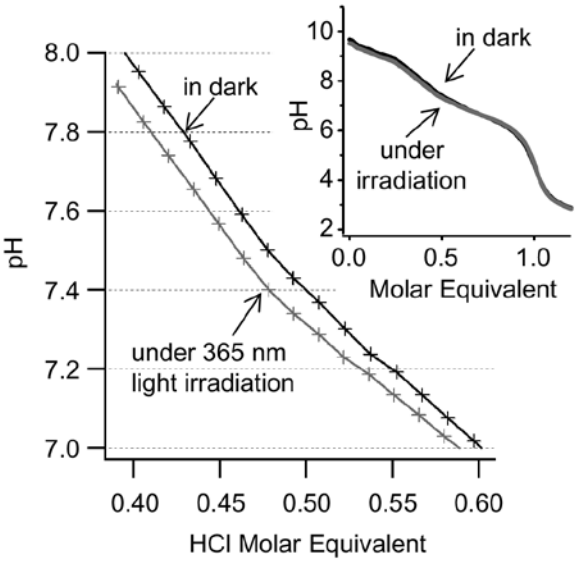

Figure 5. pH titration curves of the 91:9 mixture of **1Na** and **2** (sodium salt by addition of NaOH) in 0.1 M NaCl(aq), as measured in the dark and under 365-nm light irradiation.

pH titration curve measurement of mixed dispersion

Using a potentiometric pH titration, we measured the acid-dissociation equilibrium of the carboxyl group for dispersions composed of **1Na** (6.6 mM (91%)) and the sodium salt of **2** (0.66 mM (9%)) in 60 mL of 0.1 M NaCl(aq) under dark condition or under 365-nm light irradiation. The ratio of *trans*-isomer to *cis*-isomer was 99.8:0.2 in dark condition and 21.6:78.4 under 365-nm light irradiation, as determined via high-performance liquid chromatography (HPLC). The temperature was maintained at 25 °C by a water bath. As shown in Figure 5, the titration curve shifted left as a result of 365-nm light irradiation. This shift in the titration curve at pH 7.5 indicates that the ratio of the anion form to the protonated neutral form increases by 2% under 365-nm light irradiation.

Fourier transform infrared (FTIR) spectra of mixed dispersion

Figure 6 shows the difference absorption FTIR spectrum of the dispersion of **1Na** (6 mM (91%)) and **2** (0.6 mM (9%)) in the pH 7.3 buffered water. The absorption spectrum of the dispersion before light irradiation was subtracted from the spectrum collected after 365-nm light irradiation. The sample was loaded into a sealed CaF_2 liquid cell, and measurements were carried out under a nitrogen atmosphere. To remove the vibration–rotation signals of water vapor, water-vapor decomposition processing was applied to the obtained spectra. Even though the difference signal intensities were very small, the negative peak at 1730 cm^{-1} clearly indicated a decrease in intensity of the C=O stretching vibration of the neutral carboxylic acid group by 365-nm light irradiation. Consequently, the ratio of the anion form increased.

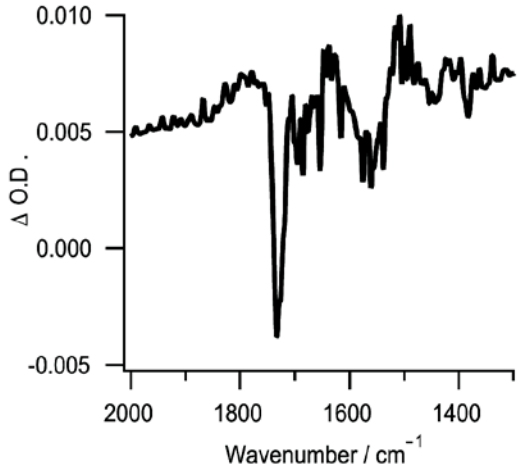

Figure 6. Difference FTIR spectrum of the mixed dispersion of **1Na** (91%) and **2** (9%) at pH 7.3; the spectrum collected before light irradiation was subtracted from the spectrum collected after 365-nm light irradiation.

Mechanism of the propagation of azobenzene photoisomerization to macroscopic motions of self-assemblies

According to the pH titration curve (Figure 5), the molar ratio of the anion form in a dispersion of **1Na** and **2** in buffered water under UV-irradiation increased; this increase was experimentally confirmed by FTIR measurements, as shown in Figure 6. On the basis of the curves shown in Figure 5, the molar ratio between the anion form and the neutral form was estimated to shift from 50:50 to 52:48 at pH 7.4 and to shift from 52:48 to 54:46 at pH 7.5 by UV-light irradiation. The 2% increase in the ratio between the anion form and the neutral form corresponds to the 0.1 increase in pH at pH 7.5, as shown in Figure 2. This fact implies that the shift in this ratio induces a change in the stable structure of macroscopic self-assemblies from helix to rod. As with this pH-induced structural change, the stable structures of the self-assemblies were changed by the light-induced anion formation: helical assemblies were recoiled to form (1) more relaxed helices with propelling motion (pH 7.4, Figure 7a), (2) rod-like assemblies with winding motion (pH 7.5, Figure 7b), or (3) invisible assemblies with tail-shaking motion (pH 7.5, Figures 3 and 7c) in pH-constant phosphate buffered water. The ability of vesicles to maintain their vesicular structure at pH 7.8 can be explained in a similar manner. Therefore, we propose that the key mechanism of the macroscopic motion is the collective deprotonation of the carboxyl groups.

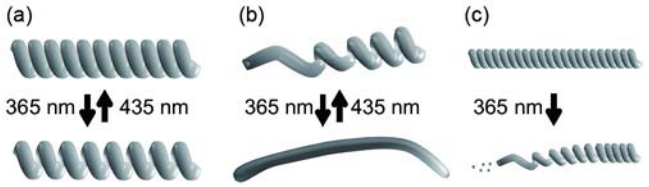

Figure 7. Illustrations of the photo-triggered morphological transformations of helical assemblies composed of **1** and **2**, which were observed in our experiments: (a) recoiling of a bold helical assembly to form a relaxed helical assembly with propelling motion under 365-nm light irradiation and its reverse reaction under 435-nm light irradiation,[12] (b) recoiling of a bold helical assembly to form a rod-like assembly under 365-nm light irradiation and its reverse reaction under 435-nm light irradiation,[12] and (c) recoiling of a thin helical assembly to produce an invisible assembly with tail-shaking motion under 365-nm light irradiation (present study).

The question of how photoirradiation leads to the deprotonation of the carboxyl group as yet remains unanswered. As previously mentioned, inhibition of deprotonation of carboxylic acid in self-assembly is caused by its association property. The increase in the effective cross-sectional area of **2** by photoisomerization results in loose packing of the component molecules. The increase in the average distance between the head-groups of the component molecules in the assembly reduces the electrostatic repulsion among carboxylate anions and encourages the deprotonation of the carboxylic acid groups.

The mechanism of the photoirradiation-triggered macroscopic motion of the assemblies is thus summarized in Figure 8. (1) UV irradiation induces the azobenzene photoisomerization from the *trans*-isomer (**2**-*trans*) to the *cis*-isomer (**2**-*cis*). (2) The increase in the effective cross-sectional area of **2**-*cis* makes the molecular distance increase to reduce electrostatic repulsion. (3) This reduction in repulsion encourages the deprotonation of the carboxylic acid group. (4) The increase in the ratio between the carboxylate anion and the neutral carboxylic acid destabilizes the original shape of the assembly, allowing it to transform into a new morphology via macroscopic motion.

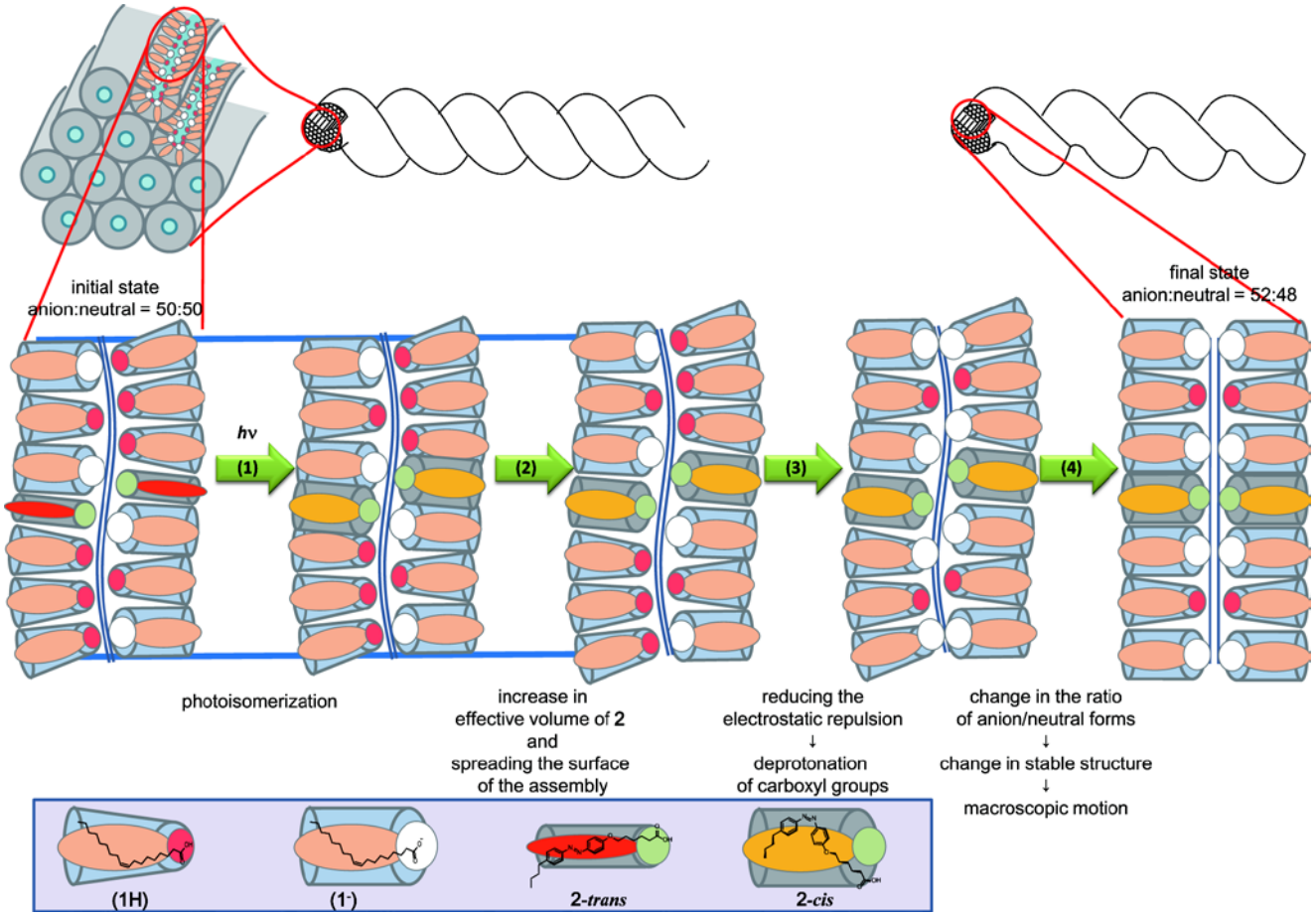

Figure 8. Schematic of the mechanism of macroscopic dynamics of the helical assemblies composed of **1** and **2** activated by photoisomerization of **2**.

Conclusions

The macroscopic dynamics of supramolecular assembly has recently begun to attract broad interest. One of the distinct points of the motions presented in this study is the fact that the minor component triggers the dynamics of mass assembly. Understanding the underlying mechanism of this type of motion requires elucidation of the dynamical collectivity in the assemblies. We proposed here that the essential step to create the macroscopic dynamics is a deprotonation reaction of the carboxyl groups of **1H** and **2** in the assembly, which cooperatively proceeds with the photoisomerization of **2** and an increase in the effective cross-sectional area of **2** (Figure 8). Because the macroscopic motion of self-assembly was triggered by the minor component, the differences before and after photoinduced motion, as detected by pH-titration and FTIR-measurements, were small. However, all of the experimental results presented in this paper support the photoisomerization-triggered deprotonation of the carboxyl groups. In numerous previous studies, morphological changes of colloidal assemblies with pH-responsive groups were achieved by external pH stimulus.[9,19] By contrast, in a life-system, biological macromolecules change their conformations via proton dissociation and association, triggered by a small internal structural change.[20] From a biomimetic viewpoint, our macroscopic dynamics, in which acid dissociation was triggered by the isomerization of an azobenzene dye present in the assembly as a minor component, is important for the construction of supramolecular machinery.

Experimental Section

General Information

For microscopic observation of the photoinduced behavior, a differential interference contrast microscope (Nikon TE2000) equipped with a mercury lamp epifluorescent unit and UV-1A and BV-1A filter units was used. Movies were recorded using a USB-CCD camera (Sentech STC-TC152USB). The movie files were edited and compacted using the Sony Vegas Movie Studio Platinum 9.0 software. Solution ^{1}H-NMR spectra were recorded on a JEOL JEX 270 spectrometer, and TMS was used as an internal reference.

Materials

Extra-pure-grade sodium oleate (**1Na**) and oleic acid (**1H**) were purchased from Junsei Chemical and were used without further purification. The azobenzene derivative 6-[4-(4-*n*-butylphenylazo)phenoxy]hexanoic acid (**2**) was used after synthesis. All other reagents and distilled water were also purchased and used without purification.

Preparation of 6-[4-(4-*n*-butylphenylazo)phenoxy]hexanoic acid (2)[12,21]

4-*n*-Butyl-4′-hydroxyazobenzene was obtained from the azocoupling reaction between 4-*n*-butylaniline and phenol and was subsequently recrystallized from hexane. The amphiphilic azobenzene 6-[4-(4-butylphenylazo)phenoxy]hexanoic acid (**2**) as obtained by etherization of 4-*n*-butyl-4′-hydroxyazobenzene with *n*-bromohexanoic acid ethyl ester to form 6-[4-(4-butylphenylazo)phenoxy]hexanoic acid ethyl ester, de-esterification, and recrystallization from ethanol. ^{1}H NMR of **2** (270 MHz, $CDCl_3$, TMS) δ = 7.89 (d, J = 8.9 Hz, 2H; Ar-H), 7.80 (d, J = 8.4 Hz, 2H; Ar-H), 7.31 (d, J = 8.4 Hz, 2H; Ar-H), 6.99 (d, J = 8.9 Hz, 2H; Ar-H), 4.05 (t, J = 6.3 Hz, 2H; OCH_2), 2.68 (t, J = 7.7 Hz, 2H; CH_2), 2.42 (t, J = 7.3 Hz, 2H; CH_2), 1.51–1.91 (m, 8H; CH_2), 1.31–1.45 (m, 2H; CH_2), 0.94 ppm (t, J = 7.3 Hz, 3H; CH_3).

General method for preparing and observing the photomotile self-assemblies

A mixed solution of $CHCl_3$ and MeOH (9:1) containing **1Na** and **2** was dispensed to a glass vial. The solvent was evaporated *in vacuo* to obtain mixed films of **1Na** (1.2 mg, 3.9 μmol) and **2** (0.12 mg, 0.33 μmol). One milliliter of 75 mM phosphate buffer solution was added to the films. The substrates were dispersed by ultrasonication for 10 min to obtain a pale-yellow dispersion. The dispersion was placed on a thin slide glass, sealed using a Frame-Seal™ slide chamber (Bio-Rad) and a cover glass, and incubated for 1 d at 25 °C. The assemblies were formed spontaneously in the sealed pool.

Assemblies in the slide glass chamber were observed using a differential interference contrast microscope (Nikon TE2000) at 25 °C, which was controlled by a homemade temperature-controlled stage. For irradiation with 365-nm light, a mercury lamp in the epifluorescent unit of the microscope and a UV-1A filter unit (the excitation filter wavelengths are between 360 and 370 nm; the wavelength of the bright line spectrum is 365–366 nm) were used. For irradiation with 435-nm light, the same lamp and a BV-1A filter unit (the excitation filter wavelengths are between 430 and 440 nm; the wavelength of the bright line spectrum is 435–436 nm) were used.

Π–A curve measurements

Sixty microliters of a mixed benzene solution of **1H** (76.3 μg mL^{-1}) and **2** (11.1 μg mL^{-1}) was deposited onto distilled water poured into a 5 cm × 20 cm trough; the surface pressure was subsequently measured at room temperature using a Wilhelmy balance (Kyowa Interface Science). For measurement of the Π–A curves under irradiation, a 365-nm LED lamp (Optocode LED-UV365P) was used.

SAXD using synchrotron microbeam X-ray radiation

μSAXD measurements for individual assemblies were carried out at the BL-4A beamline at PF-KEK in Japan. The incident beam was monochromated with a multilayer mirror to be 10 keV and was focused to smaller than 5 μm × 5 μm by Kirkpatrick–Baez mirrors.[22] To control the focus and the area of the X-ray beam, an optical microscope system was used. The aqueous sample, prepared in the same manner as previously described as a general method for preparation, was placed onto a thin glass slide (Matsunami NEO Cover Glass No. 00; thickness: 0.06–0.08 mm) and sealed using a frame-seal incubation chamber. Two-dimensional (2D) images of μSAXD patterns were recorded with a 1024 × 1024-pixel IICCD camera (Hamamatsu). To calculate the *d*-spacing from the 2D images, silver behenate diffraction peaks were used as an external reference.[23]

Potentiometric pH titration

An automatic volumetric titrator (Metrohm 877 Titrino Plus) equipped with a pH combination electrode (Lutron PE-11) was used for potentiometric pH titrations. Titrant HCl solution was standardized to 0.534 M using a Na_2CO_3 standard solution as a reference. A clear dispersion of a mixture of **1** (240 mg, 788 μmol) and **2** (29.1 mg, 79 μmol) in 120 mL of 0.1 M NaCl(aq) containing 79 μmol of NaOH was prepared using an ultrasonicator, and the resulting dispersion was dispensed into two 50-mL test tubes. Samples were incubated at 25 °C for approximately 10 min in a water incubation bath, and titrant was added slowly (by 10-μL stepwise additions) to the test tubes under continuous, vigorous stirring to obtain the titration curve data. One of the samples was photoirradiated by a 365-nm handy LED lamp before and during measurement. The method for the pH titration for **1** has been reported previously.[13]

HPLC

A clear dispersion of a mixture of **1** (240 mg, 788 μmol) and **2** (29.1 mg, 79 μmol) in 120 mL of 0.1 M NaCl(aq) containing 79 μmol of NaOH was prepared using an ultrasonicator, and 50 mL of the resulting dispersion was dispensed into two test tubes. One sample was photoirradiated using a 365-nm LED lamp. Then, each 5 μL of the solution was loaded into an HPLC system (JASCO, LC2000) equipped with an octadecylsilane (ODS) column (Nacalai Tesque, Cosmosil 5C_{18}-AR-II) and a UV detector (JASCO, UV2075). The eluent was a 9:1 mixed solution of methanol and 0.05% (v/v) trifluoroacetic acid aqueous solution, and the wavelength of the detector was λ = 306 nm (an isosbestic point of *trans* and *cis* isomers of **2**).

FTIR measurements

The dispersion of **1Na** (6 mM (91%)) and **2** (0.6 mM (9%)) in pH 7.3 phosphate-buffered water was placed on a CaF_2 crystal and sealed using a 12-μm-thick polymer spacer. The chamber of the FTIR spectrometer was purged with dry N_2 gas. FTIR measurements were carried out before and after the samples were irradiated with 365-nm light, and the difference spectra were obtained. To remove the vibration–rotation spectrum of water, the vapor-decomposition plug-in for the JASCO software was used.

Acknowledgements

This work was funded by JST PRESTO (Molecular Technology) from MEXT Japan. Microbeam SAXD experiments were performed with approval of the Photon Factory Program Advisory Committee (Proposal no. 2012G747). Y.K. would like to thank Dr. Tetsunari Kimura and Dr. Minoru Kubo (RIKEN) for useful suggestions for the FTIR measurements, and Mr. A. Miyazaki and Mr. N. Tanigake for their contribution in the experiments.

Keywords: Molecular devices • Supramolecular chemistry • Photochromism • Protonation • Carboxylic acid

[1] a) G. Zhao and M. Pumera, *Chem.-Asian J.* **2012**, *7*, 1994-2002; b) M. M. Boyle, R. A. Smaldone, A. C. Whalley, M. W. Ambrogio, Y. Y. Botros and J. F. Stoddart, *Chem. Sci.* **2011**, *2*, 204-210; c) M. von Delius and D. A. Leigh, *Chem. Soc. Rev.* **2011**, *40*, 3656-3676; d) E. R. Kay, D. A. Leigh and F. Zerbetto, *Angew. Chem. Int. Ed.* **2007**, *46*, 72-191.

[2] a) D. Bleger, Z. Yu and S. Hecht, *Chem. Commun.* **2011**, *47*, 12260-12266; b) F. Ercole, T. P. Davis and R. A. Evans, *Polymer Chemistry* **2010**, *1*, 37-54; c) M. L. Bossi and P. F. Aramendia, *J. Photochem. Photobiol., C* **2011**, *12*, 154-166; d) T. Kim, L. Y. Zhu, R. O. Al-Kaysi and C. J. Bardeen, *Chemphyschem* **2014**, *15*, 400-414.

[3] a) S. Kobatake, S. Takami, H. Muto, T. Ishikawa and M. Irie, *Nature* **2007**, *446*, 778-781; b) K. Uchida, S. I. Sukata, Y. Matsuzawa, M.

Akazawa, J. J. D. de Jong, N. Katsonis, Y. Kojima, S. Nakamura, J. Areephong, A. Meetsma and B. L. Feringa, *Chem. Commun.* **2008**, 326-328; c) M. Morimoto and M. Irie, *J. Am. Chem. Soc.* **2010**, *132*, 14172-14178; d) D. Kitagawa, H. Nishi and S. Kobatake, *Angew. Chem. Int. Ed.* **2013**, *52*, 9320-9322.

[4] H. Koshima, K. Takechi, H. Uchimoto, M. Shiro and D. Hashizume, *Chem. Commun.* **2011**, *47*, 11423-11425.

[5] a) H. Koshima, N. Ojima and H. Uchimoto, *J. Am. Chem. Soc.* **2009**, *131*, 6890-6891; b) O. S. Bushuyev, *J. Am. Chem. Soc.* **2013**, *135*, 12556-12559; c) N. K. Nath, L. Pejov, S. M. Nichols, C. H. Hu, N. Saleh, B. Kahr and P. Naumov, *J. Am. Chem. Soc.* **2014**, *136*, 2757-2766.

[6] a) A. Priimagi, C. Barrett and A. Shishido, *J. Mater. Chem. C* **2014**, *2*, 7155-7162; b) T. Ube and T. Ikeda, *Angew. Chem. Int. Ed.* **2014**, *53*, 10290-10299.

[7] a) T. Ikegami, Y. Kageyama, K. Obara and S. Takeda, *Angew. Chem. Int. Ed.* **2016**, *55,* 8239-8243; b) T. Ikegami, Y. Kageyama and S. Takeda in *Abstracts of The 2015 International Chemical Congress of Pacific Basin Societies,* Honolulu, HI, USA, **2015**, PHYS0921.

[8] a) S. Serak, N. Tabiryan, R. Vergara, T. J. White, R. A. Vaia and T. J. Bunning, *Soft Matter* **2010**, *6*, 779-783; b) T. J. White, N. V. Tabiryan, S. V. Serak, U. A. Hrozhyk, V. P. Tondiglia, H. Koerner, R. A. Vaia and T. J. Bunning, *Soft Matter* **2008**, *4*, 1796.

[9] a) P. Brown, C. P. Butts and J. Eastoe, *Soft Matter* **2013**, *9*, 2365-2374; b) Z. Chu, C. A. Dreiss and Y. Feng, *Chem. Soc. Rev.* **2013**, *42*, 7174-7203.

[10] K. Higashiguchi, G. Taira, J. Kitai, T. Hirose and K. Matsuda, *J. Am. Chem. Soc.* **2015**, *137*, 2722-2729.

[11] a) T. Hamada, R. Sugimoto, M. C. Vestergaard, T. Nagasaki and M. Takagi, *J. Am. Chem. Soc.* **2010**, *132*, 10528-10532; b) T. Hamada, Y. T. Sato, K. Yoshikawa and T. Nagasaki, *Langmuir* **2005**, *21*, 7626-7628.

[12] Y. Kageyama, N. Tanigake, Y. Kurokome, S. Iwaki, S. Takeda, K. Suzuki and T. Sugawara, *Chem. Commun.* **2013**, *49*, 9386-9388.

[13] Y. Kageyama, T. Ikegami, N. Hiramatsu, S. Takeda and T. Sugawara, *Soft Matter* **2015**, *11*, 3550-3558.

[14] a) K. Morigaki and P. Walde, *Curr. Opin. Colloid Interface Sci.* **2007**, *12*, 75-80; b) J. R. Kanicky and D. O. Shah, *J. Colloid Interface Sci.* **2002**, *256*, 201-207; c) J. R. Kanicky, A. F. Poniatowski, N. R. Mehta and D. O. Shah, *Langmuir* **2000**, *16*, 172-177; d) M. Ishimaru, T. Toyota, K. Takakura, T. Sugawara and Y. Sugawara, *Chem. Lett.* **2005**, *34*, 46-47; e) K. Edwards, M. Silvander and G. Karlsson, *Langmuir* **1995**, *11*, 2429-2434; f) D. P. Cistola, J. A. Hamilton, D. Jackson and D. M. Small, *Biochemistry* **1988**, *27*, 1881-1888. g) D. P. Cistola, D. Atkinson, J. A. Hamilton and D. M. Small, *Biochemistry* **1986**, *25*, 2804-2812.

[15] S. Salentinig, L. Sagalowicz and O. Glatter, *Langmuir* **2010**, *26*, 11670-11679.

[16] M. Mulqueen and P. D. T. Huibers *Measuring Equilibrium Surface Tensions*, in *Handbook of Applied Surface and Colloid Chemistry* Vol. 2 (Ed. K. Holmberg), John Wiley & Sons Ltd, West Sussex, **2002**, 217-224.

[17] Strictly speaking, the cross-sectional areas should be compared with consideration of the molecular pressure present in self-assemblies. Even though the strength of molecular packing was assumed to decrease after UV irradiation on the basis of the easier deformation behavior of UV-irradiated assemblies under X-ray irradiation observed in our synchrotron microbeam SAXD measurements, we do not know the strength of the molecular pressure in each shape of assembly.

[18] The A_0 of oleic acid in pH 2 buffer has been reported as 0.40 nm^2 in (a) and 0.41 nm^2 in (b). We attributed the differences between our experimental value and the reported values to the deprotonation of carboxylic acid in our study. (a) T. Baba, K. Takai, T. Takagi and T. Kanamori, *Chem. Phys. Lipids* **2013**, *172–173*, 31-39. (b) M. Tomoaia-Cotişel, J. Zsakó, A. Mocanu, M. Lupea and E. Chifu, *J. Colloid Interface Sci.* **1987**, *117*, 464-476.

[19] a) Y. I. Gonzalez, H. Nakanishi, M. Stjerndahl and E. W. Kaler, *J. Phys. Chem. B* **2005**, *109*, 11675-11682; b) J. Zhou, L. Wang, Q. Yang, Q. Liu, H. Yu and Z. Zhao, *J. Phys. Chem. B* **2007**, *111*, 5573-5580; c) L. A. Connal, Q. Li, J. F. Quinn, E. Tjipto, F. Caruso and G. G. Qiao, *Macromolecules* **2008**, *41*, 2620-2626; d) A. Pal and J. Dey, *Soft Matter* **2011**, *7*, 10369-10376; e) K. Suzuki, K. Kurihara, Y. Okura, T. Toyota and T. Sugawara, *Chem. Lett.* **2012**, *41*, 1084-1086; f) B. H. Morrow, P. H. Koenig and J. K. Shen, *Langmuir* **2013**, *29*, 14823-14830; g) A. Car, P. Baumann, J. T. Duskey, M. Chami, N. Bruns and W. Meier, *Biomacromolecules* **2014**, *15*, 3235-3245; h) A. Uesaka, M. Ueda, A. Makino, T. Imai, J. Sugiyama and S. Kimura, *Langmuir* **2014**, *30*, 1022-1028; i) H. Wang, B. Tan, J. Wang, Z. Li and S. Zhang, *Langmuir* **2014**, *30*, 3971-3978; j) A. Arnould, C. Gaillard and A.-L. Fameau, *J. Colloid Interface Sci.* **2015**, *458*, 147-154; k) A.-L. Fameau, A. Arnould and A. Saint-Jalmes, *Curr. Opin. Colloid Interface Sci.* **2014**, *19*, 471-479.

[20] a) V. K. Rastogi and M. E. Girvin, *Nature* **1999**, *402*, 263-268; b) H.-W. Choe, Y.-J. Kim, J.-H. Park, T. Morizumi, E. F. Pai, N. Krauss, K. P. Hofmann, P. Scheerer and O. P. Ernst, *Nature* **2011**, *471*, 651-655; c) K. Gerwert, G. Souvignier and B. Hess, *Proc. Natl. Acad. Sci. U. S. A.* **1990**, *87*, 9774-9778; d) A. B. Woehri, G. Katona, L. C. Johansson, E. Fritz, E. Malmerberg, M. Andersson, J. Vincent, M. Eklund, M. Cammarata, M. Wulff, J. Davidsson, G. Groenhof and R. Neutze, *Science* **2010**, *328*, 630-633.

[21] D. Stewart and C. T. Imrie, *J. Mater. Chem.* **1995**, *5*, 223-228.

[22] Y. Nozue, R. Kurita, S. Hirano, N. Kawasaki, S. Ueno, A. Iida, T. Nishi and Y. Amemiya, *Polymer* **2003**, *44*, 6397-6405.

[23] T. C. Huang, H. Toraya, T. N. Blanton and Y. Wu, *J. Appl. Cryst.* **1993**, *26*, 180-184.